New Thiophene-Linked Conjugated Poly(azomethine)s: Theoretical Electronic Structure, Synthesis, and Properties

Fu-Chuan Tsai,[†] Chao-Ching Chang,[†] Cheng-Liang Liu,[†] Wen-Chang Chen,*[,†] and Samson A. Jenekhe*[,‡]

Department of Chemical Engineering and Institute of Polymer Science and Engineering, National Taiwan University, Taipei, Taiwan 106, and Departments of Chemical Engineering and of Chemistry, University of Washington, Seattle, Washington 98195-1750

Received September 14, 2004; Revised Manuscript Received December 20, 2004

ABSTRACT: We report a joint theoretical and experimental study of several new thiophene-based poly(azomethine)s. Hybrid density functional theory (DFT) method was used to calculate the optimized geometry and electronic structure of poly(azomethine)s. Theoretical band gaps of the new thiophene-based poly(azomethine)s were in the range 2.33−2.67 eV, which are smaller than that of the phenylene-based polymer. The variation of the backbone ring (fluorene, carbazole, or naphthalene) or donor/acceptor side group on the phenylene ring significantly affected the dihedral angles and resulted in the variation of electronic properties (ionization potential, electron affinity, and band gap) of the poly(azomethine)s. Five soluble new conjugated poly(azomethine)s derived from the polymerization of 2,5-diformyl-3-hexylthiophene (**DFHT**) with various diamines were prepared and characterized. The optical and electrochemical band gaps of the polymer films were in the ranges 2.21−2.28 and 2.13−2.24 eV, respectively. The trend of the effect of the backbone ring or side chain on the experimental electronic properties is in good agreement with the theoretical results. Our study demonstrates how the electronic properties of conjugated poly(azomethine)s can be tuned by the backbone ring or side group, which could be important for electronic or optoelectronic applications of the materials.

Introduction

Conjugated polymers have been widely recognized as a new class of molecular semiconductors for electronic and optoelectronic devices, such as light emitting diodes,[1] thin film transistors,[2] and photovoltaic cells.[3] We are particularly interested in conjugated poly(azomethine)s due to their documented excellent thermal, mechanical, electronic, optical, optoelectronic, and fiber-forming properties.[4−16] The general chemical structure of conjugated poly(azomethine)s is $[-(Ar_1)-CH{=}N-(Ar_2)-N{=}CH-]_n$. The C=N linkages of poly(1,4-phenylenemethylidyneitrilo-1,4-phenylenenitrilomethylidyne) (**PPI**) are isoelectronic with the C=C linkages of poly(*p*-phenylene vinlyene) (**PPV**) and result in a significant difference in the electronic and optoelectronic properties.[5] **PPI**, like **PPV**, is insoluble in organic solvents. However, it is soluble in protonic acids or via the methodology of reversible Lewis acid−base complexation with gallium chloride in organic solvents.[5] The solubility of conjugated poly(azomethine)s has been improved by introducing flexible alkyl or alkoxy side groups on the aromatic rings.[7−14]

Soluble conjugated poly(azomethine)s provide the opportunity of correlating chemical structure with their electronic, optical, and optoelectronic properties, such as band gap,[5a,5d,8c,9b] refractive index,[5b,5c] nonlinear optical properties,[5e] luminescence characteristics,[5e,8c,16] and charge carrier mobility.[15] It has been shown that the electronic properties of conjugated poly(azomethine)s could be varied through different backbone rings, electron donating/accepting side group substitution, intramolecular hydrogen bonding, or complexation.[5a,d] Destri and co-workers have shown that the band gap of conjugated poly(azomethine)s was significantly reduced by the regular alternation of sequences of thienylene and phenylene segments with various segment lengths.[8] These polymers showed evidence of electronic confinement in the thienylene fragments and were of interest as possible multiple quantum wires/wells. Wang et al. prepared similar conjugated poly(azomethine)s with alkyl chain substituted terthiophene building block.[9b] Recently, the light-emitting properties of thiophene-based conjugated poly(azomethine)s were reported.[16b]

Although the tuning of the electronic structure through the variation of side chain or backbone of conjugated poly(azomethine)s has been extensively reported,[4−16] a joint theoretical and experimental study has not been reported yet. Theoretical analysis of the electronic structure of conjugated polymers can establish the relationships between polymer structure and electronic and optoelectronic properties.[17−27] However, a systematic theoretical study of the electronic properties of soluble conjugated poly(azomethine)s has so far not been reported as far as we know.

In this paper, theoretical analysis on seven soluble conjugated poly(azomethine)s containing the thiophene ring, as shown in Chart 1, is reported. Different backbone ring or electron donating/withdrawing side groups were introduced to investigate their effects on the electronic structure. The theoretical ground-state geometry and electronic structure of the poly(azomethine)s were optimized by the hybrid density functional theory (DFT) under the periodic boundary conditions at the B3LYP level and 6-31G basis set. The theoretical electronic properties were verified by comparison with experimental results on five soluble conjugated poly-

* Corresponding authors: E-mail: (W.-C.C.) chenwc@ntu.edu.tw; (S.A.J) jenekhe@u.washington.edu.

[†] Department of Chemical Engineering and Institute of Polymer Science and Engineering, National Taiwan University.

[‡] Departments of Chemical Engineering and of Chemistry, University of Washington.

10.1021/ma048112o CCC: $30.25
Published on Web 02/09/2005

Chart 1

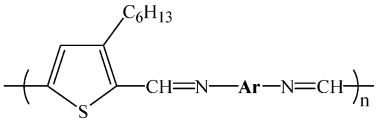

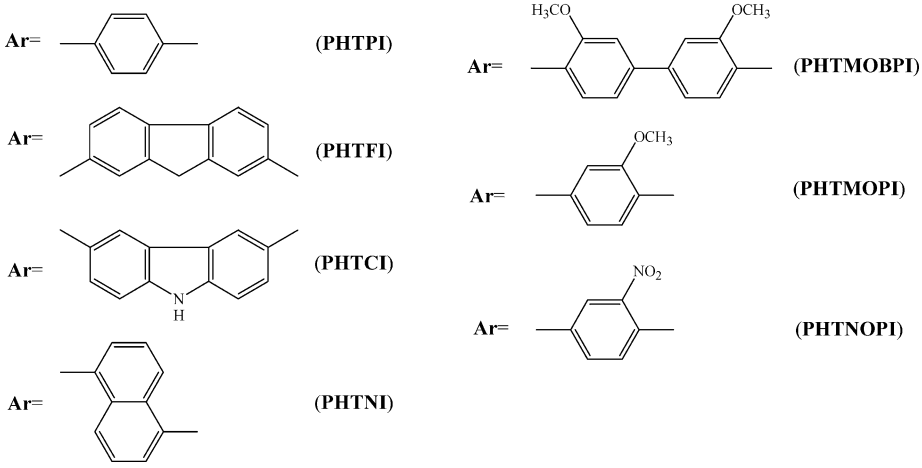

(azomethine)s, which were synthesized by polymerization of 2,5-diformyl-3-hexylthiophene (**DFHT**) with various diamines. The molecular structures, thermal, optical, electronic, and electrochemical properties of the new poly(azomethine)s were investigated in detail.

Theoretical Analysis

Theoretical Methodology. The ground-state geometry and electronic structure of the poly(azomethine)s were optimized by the hybrid density functional theory (DFT) method using periodic boundary conditions at the B3LYP level (Becke-style 3-Parameter Density Functional Theory, using the Lee−Yang−Parr correlation functional) with 6-31G basis set performed on Gaussion03 program package.[28] This method, B3LYP//B3LYP (started with B3LYP geometry optimization followed by B3LYP electronic structure calculation), is more reliable than other methodologies when applied to a system where the equilibrium geometries deviate substantially from planar structures.[18b]

In this analysis, one full unit cell was used for the calculation of an isolated, infinite, and one-dimensional polymer in the gas phase, starting from the geometry of the central portion (two repeat units) of the corresponding polymer. Full geometry optimization was performed inside a given lattice length, and the lattice parameters were then varied to locate both the equilibrium lattice parameters and the lowest-energy structure in that unit cell.

The theoretical electronic structure of the polymers in Chart 1 treated without the 3-hexyl side-group revealed no significant difference in comparison with that with the side group. For example, the electronic structure properties (IP, EA, E_g) of **PHTPI** are 5.15, 2.76, and 2.39 eV, respectively. In comparison, these values would be 5.32, 2.97, and 2.35 eV, respectively, if it was treated without the 3-hexyl side-group. It suggests that the 3-hexyl side-group contributes to the destabilization of the frontier levels but affects the band gap weakly. Since the calculation of the polymer with long side-group substitution was time-consuming, the calculation of the theoretical electronic structures of the polymers in Chart 1 was treated without the 3-hexyl side-group.

Experimental Section

Materials. 1,4-Phenylenediamine (Aldrich, 97%) was purified by sublimation. 2,5-Dibromo-3-hexylthiophene (Aldrich, 97%), 2,7-diaminofluorene (TCI, 97%), 3,6-diaminocarbazole (TCI, 98%), 3,3′-dimethoxy-biphenyl-4,4′-diamine (Lancaster, 99.7%), 1,5-diaminonaphthalene (TCI, 97%), *n*-butyllithium (Aldrich, 1.6 M in hexane), lithium chloride (Aldrich, 99.99%), *N*,*N*-dimethylformamide (DMF) (Aldrich, anhydrous 99.8%), 1-methyl-2-pyrrolidone (NMP) (Aldrich, anhydrous 99.5%), dimethyl sulfoxide (DMSO) (Acros, 99.7%), hexamethylenephosphoramide (HMPA) (Aldrich, 99%), and diethyl ether (Tedia, 99.9% anhydrous) were used as received.

Synthesis of Monomers and Polymers. 2,5-Diformyl-3-hexylthiophene (DFHT). DFHT was prepared with a procedure similar to that reported in the literature,[29] as shown in Scheme 1. A solution of 5 g (15.33 mmol) of 2,5-dibromo-3-hexylthiophene in 400 mL of ether was added to 68.3 mL of a solution of *n*-BuLi in *n*-hexane (1.6 M) in a dry ice/acetone bath by a syringe under nitrogen atmosphere. The mixture was stirred for 5 min at −78 °C, and then 11.5 mL of DMF was added. After the mixture was stirred for 1 h, the dry ice/acetone bath was removed and the reaction mixture was allowed to warm gradually to room temperature. The product was extracted with 200 mL of water, and the aqueous layer was extracted once with ether. The organic layers were dried over anhydrous sodium sulfate, and the solvent was then removed by rotary evaporation to afford the crude product. It was purified by silica gel chromatography (*n*-hexane: CH_2Cl_2 = 1:2) twice to afford 1.26 g of yellow oil product (37% yield). ^{1}H NMR ($CDCl_3$), δ (ppm): 10.15 (1H), 9.98, (1H), 7.66 (1H), 3.01 (2H), 1.71 (2H), 1.40−1.31 (6H), 0.90 (3H). ^{13}C NMR ($CDCl_3$), δ (ppm): 13.97, 22.45, 28.46, 28.83, 31.13, 31.44, 137.14, 143.25, 147.83, 151.98, 182.96, 183.35.

Synthesis of Polymers. Conjugated poly(azomethine)s were synthesized using a method similar to that reported in the literature,[5b,5c] as shown in Scheme 1. All the polymers were prepared by solution condensation polymerization of the **DFHT** with aromatic diamines in HMPA/NMP (1:1 by volume) with LiCl as the water removal reagent under nitrogen purge. The mixture was poured into methanol after 48−72 h of reaction time. The product was reprecipitated twice in THF/hexane if it is soluble in THF. All the products were cleaned by an overnight extraction with refluxing methanol in a

Scheme 1. Synthesis of the Monomer DFHT and Soluble Conjugated Poly(azomethine)s

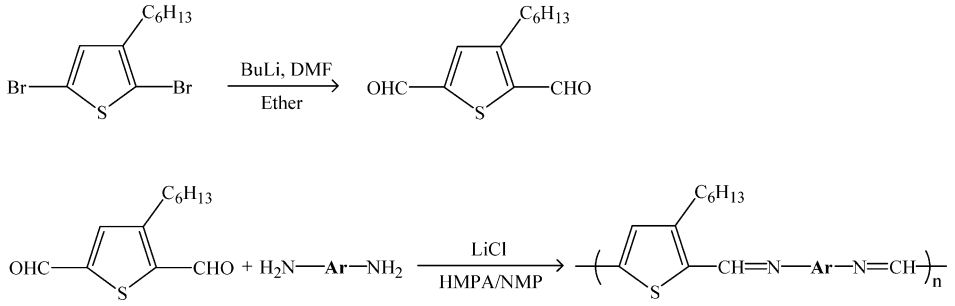

Soxhlet apparatus. After that, the polymers were dried overnight in a vacuum at 60 °C. A brief description of the preparation of each polymer follows.

PHTPI. DFHT (0.96 g, 4.28 mmol) was reacted with 1,4-phenylenediamine (0.46 g, 4.28 mmol) in 20 mL of 1:1 HMPA/NMP containing 0.8 g of LiCl under nitrogen purge at room temperature. A red product was precipitated by pouring into 500 mL of stirring methanol after 48 h reaction time (1.01 g, 80% yield). Anal. Calcd for $(C_{18}H_{20}N_2S)_n$: C, 72.93; H, 6.80; N, 9.45; S, 10.82. Found: C, 72.93; H, 6.98; N, 9.02; S, 10.41. ^{1}H NMR (1,1,2,2-tetrachloroethane-d_2), δ (ppm): 8.62 (1H), 8.52, (1H), 7.31 (1H), 7.27 (4H), 2.78 (2H), 1.60−1.25 (6H), 0.83 (3H).

PHTFI. DFHT (0.63 g, 2.81 mmol) was reacted with 2,7-diaminofluorene (0.55 g, 2.81 mmol) in 15 mL of 1:1 HMPA/NMP containing 0.60 g of LiCl under nitrogen purge at room temperature. A red product was precipitated by pouring into 500 mL of stirring methanol after 48 h reaction time. The polymer is a red powder (0.68 g, 63% yield). Anal. Calcd for $(C_{25}H_{24}N_2S)_n$: C, 78.09; H, 6.29; N, 7.28; S, 8.34. Found: C, 77.64; H, 6.49; N, 7.22; S, 8.02. ^{1}H NMR (THF-d_8), δ (ppm): 8.89 (1H), 8.76, (1H), 7.82 (1H), 7.53−7.34 (6H), 3.98 (2H), 3.03 (2H), 1.45−1.37 (6H), 0.92 (3H).

PHTCI. DFHT (0.80 g, 3.57 mmol) was reacted with 3,6-diaminocarbazole (0.70 g, 3.57 mmol) in 20 mL of 1:1 HMPA/NMP containing 0.60 g of LiCl under nitrogen purge at room temperature. The product was precipitated by pouring into 500 mL of stirring methanol after a 48 h reaction time. The polymer is an orange powder (0.92 g, 67% yield). Anal. Calcd for $(C_{24}H_{22}N_3S)_n$: C, 74.77; H, 6.01; N, 10.9; S, 8.32. Found: C, 72.9; H, 6.13; N, 10.12; S, 8.01. ^{1}H NMR (THF-d_8), δ (ppm): 10.41 (1H), 8.96 (1H), 8.80 (1H), 8.23−7.23 (7H), 2.98 (2H), 1.47−1.37 (6H), 0.91 (3H).

PHTNI. DFHT (0.433 g, 1.93 mmol) was reacted with 1,5-diaminonaphthalene (0.315 g, 1.93 mmol) in 15 mL of 1:1 HMPA/NMP containing 0.60 g LiCl at room temperature for 54 h, and then heated to 45 °C for 18 h for further reaction. The polymer is an orange powder (0.134 g, 20% yield). Anal. Calcd for $(C_{22}H_{22}N_2S)_n$: C, 76.30; H, 6.36; N, 8.09; S, 9.25. Found: C, 74.75; H, 6.73; N, 7.68; S, 9.19. ^{1}H NMR (THF-d_8), δ (ppm): 8.85(1H), 8.41 (1H), 7.85−6.71 (7H), 3.01 (2H), 1.46−1.37 (6H), 0.91 (3H).

PHTMOBPI. DFHT (0.532 g, 2.37 mmol) was reacted with 3,3′-dimethoxy-biphenyl-4,4′− diamine (0.581 g, 2.37 mmol) in 17 mL of 1:1 HMPA/NMP containing 0.34 g LiCl at room temperature for 48 h to afford an orange powder (0.646 g, 63% yield). Anal. Calcd for $(C_{26}H_{28}N_2SO_2)_n$: C, 72.22; H, 6.48; N, 6.48; S, 7.41. Found: C, 71.42; H, 6.83; N, 6.49; S, 7.33. ^{1}H NMR (THF-d_8), δ (ppm): 8.93 (1H), 8.79 (1H), 7.42 (1H), 7.33−7.20 (6H), 3.97 (6H), 2.91 (2H), 1.44−1.37 (6H), 0.92 (3H).

Characterization. ^{1}H NMR spectra were recorded on a Bruker AVANCE 500 MHz spectrometer using chloroform-d, THF-d_8, and 1,1,2,2-tetrachloroethane-d_2 as the solvent. FTIR spectroscopy was done using a DIGILAB FTS 3500GX FT-IR spectrometer. The elemental analysis of the polymers was performed by using a HERAEUS VarioEL elemental analyzer. The molecular weights were determined on a gel permeation chromatography (GPC) (Lab Alliance solvent delivery system, Schambeck SFD Gmbh model RI2000 refractive index detector, and PLgel 5 μm MIXED-C and -D columns) at 40 °C with a THF flow rate of 1.0 mL/min. The calibration was created with polystyrene standards.

Thermogravimetric analysis (TGA) and differential scanning calorimetry (DSC) of the polymers was conducted on a TA Instruments Q50 TGA and Q100 DSC, respectively. A heating rate of 10 °C/min under flowing N_2 was used. Optical absorption spectra and photoluminescence spectra were obtained by using Jasco model V-570 and model FP-6200 spectrometers, respectively.

The fluorescence quantum efficiency of each polymer in solution was measured by excitation of the respective polymer solution and compared with the solution emission of quinine sulfate in 1 N H_2SO_4 (standard, $\phi_{PL} = 0.546$).[30] The quantum efficiency of the unknown polymer solution is related to that of the standard by eq 1.

$$\phi_u = \left[\frac{A_s F_u n^2}{A_u F_s n_s^2}\right]\phi_s \qquad (1)$$

where u subscript means the unknown and s the standard and other symbols have the following meanings: A is absorbance, ϕ is quantum efficiency, F is the integrated area, and n is index of refraction of the solvent. Absorbance of the unknown samples and the standard should be similar and small (<0.10).

The electrochemical properties of the polymer films were investigated on a Princeton Applied Research model 273A potentiostat/galvanostat with a 0.1 M acetonitrile (99.5+%, Tedia) solution containing tetrabutylammonium tetrafluoroborate ((TBA)BF_4) (Fluka, >99.9%) as the electrolyte. Platinum wire and rod-tip electrodes were used as counter and working electrodes, respectively. Silver/silver ion (Ag in 0.1 M $AgNO_3$ (Acros, 99.8%) in the supporting electrolyte solutions) was used as a reference electrode. A 3 wt % solution of a polymer in THF or DMSO was used to prepare the polymer film on the Pt rod-tip electrode. Then, the cyclic voltammetry of films was performed on a three-electrode cell. The reference electrode was calibrated through by the cyclic voltammetry of ferrocene without any polymer added into the solution. The cyclic voltammograms were obtained at a voltage scan rate of 50 mV/s. The potential values obtained vs Fc^+/Fc standard were converted to the saturated calomel electrode (SCE) scale by adding a constant voltage to them. The energy parameters EA and IP were estimated from the measured redox potentials on the basis of the prior work on conjugated polymers which has shown that: IP = $[E_{on}]^{ox}$ + 4.4 and EA = $[E_{on}]^{red}$ + 4.4, where the onset potentials are in volts (vs SCE) and IP and EA are in electronvolts. The 4.4 eV constant in the relation among IP, EA, and redox potentials is the SCE energy level vs vacuum.[31]

Results and Discussion

Geometry and Electronic Structure of PPI and PHTPI. The optimized geometries of **PPI** and **PHTPI** are shown in Figure 1. The average C−C bond length (R_{C1-C2})between the C═N linkage and phenylene ring in **PPI** is 1.463 Å while that between the C═N linkage and thiophene ring in **PHTPI** is 1.435 Å. The C═N bond lengths ($R_{C2=N}$)of **PPI** and **PHTPI** are 1.293 and 1.297

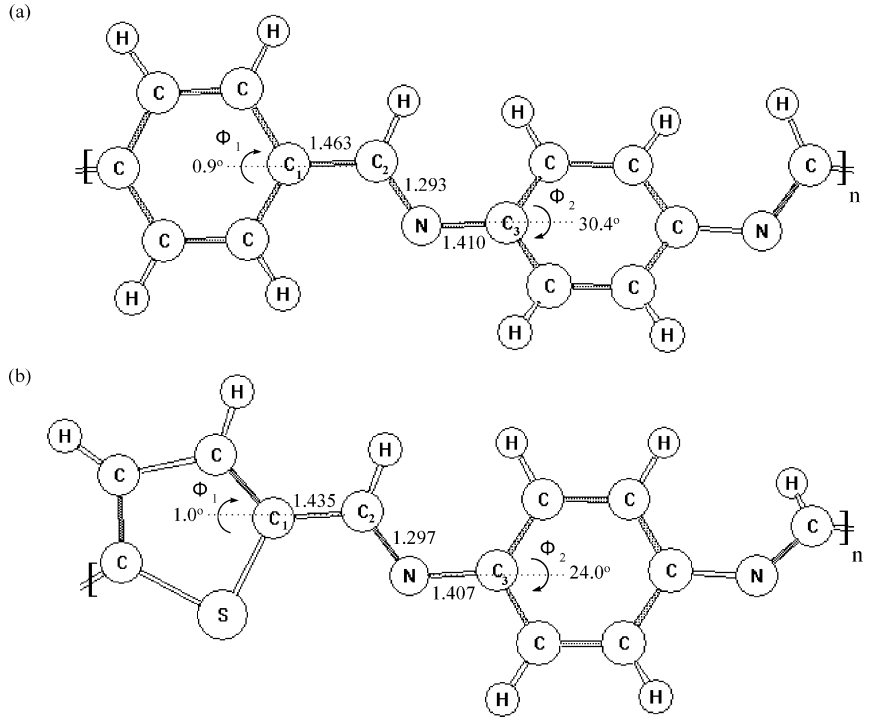

Figure 1. Optimized geometries of (a) **PPI** and (b) **PTPI**.

Table 1. Calculated Bond Lengths, Bond Length Alternation (δ_r), Dihedral Angles (Φ_1, Φ_2), and Electronic Structure (IP, EA, and E_g) of Poly(azomethine)s

	R_{C1-C2}[a] (Å)	$R_{C2=N}$[a] (Å)	R_{C3-N}[a] (Å)	δ_r[b] (Å)	R_S[c] (Å)	Φ_1[d] (deg)	Φ_2[d] (deg)	IP (eV)	EA (eV)	E_g (eV)
PPI	1.463	1.293	1.410	0.170		0.9	30.4	5.47	2.63	2.84
PHTPI	1.435	1.297	1.407	0.138	1.389	1.0	24.0	5.32	2.97	2.35
PHTFI	1.436	1.297	1.408	0.139		1.2	26.0	5.16	2.74	2.42
PHTCI	1.436	1.296	1.411	0.140		1.9	26.2	5.05	2.38	2.67
PHTNI	1.437	1.296	1.407	0.141		0.8	30.6	5.16	2.66	2.50
PHTMOBPI	1.435	1.297	1.403	0.138	1.404	1.4	15.4	5.25	2.83	2.42
PHTMOPI	1.435	1.299	1.402	0.136	1.399	1.8	27.3	5.29	2.96	2.33
PHTNOPI	1.436	1.293	1.394	0.143	1.391	2.6	37.3	6.02	3.36	2.66

[a] R_{C1-C2}, $R_{C2=N}$, and R_{C3-N} are defined in Figure 1. [b] ($R_{C1-C2}-R_{C2=N}$). [c] Carbon−carbon bond length in the phenylene ring adjacent to side chain substitution, as shown in r(12,13) of the Supporting Information. [d] Average value.

Å, respectively. Hence, bond length alternation (δ_r) between C−C and C=N is larger in **PPI** (0.170 Å) than that in **PHTPI** (0.138 Å). As shown in Figure 1, the torsional angles (Φ_1) between the C=N linkage and the adjacent phenylene ring in **PPI** and thiophene in **PHTPI** are 0.9 and 1.0°, respectively. However, a significant difference is shown on the torsional angles (Φ_2) between the C=N linkage and the adjacent *N*-phenylene ring. **PPI** has a larger Φ_2 of 30.4 ± 1.5°, as compared with that (24.0 ± 1.5°) of **PHTPI**, by 6.4°, which suggests that **PHTPI** has a more planar conformation than **PPI**. The nonplanarity of **PPI** is mostly due to the conjugation between the imine nitrogen lone pair electron and the π−electron of the *N*-phenylene ring.[4,5c] The replacement of the phenylene ring with the thiophene ring results in the reduction of steric hindrance and hence enhances the π−electron delocalization,[9a] which significantly affects the electronic structure.

Table 1 lists the theoretical electronic structure parameters of the polymers. The calculated band gaps (E_g) of **PPI** and **PHTPI** are 2.84 and 2.35 eV, respectively. The theoretical band gap of **PPI** is in a fairly good agreement with the reported experimental value.[5a] The smaller band gap of **PHTPI** than that of **PPI** is probably due to the smaller dihedral angle Φ_2 and smaller bond length difference between C−C and C=N. The theoretical ionization potential (IP) and electronic affinity (EA) of **PPI** are 5.47 and 2.63 eV while those of **PHTPI** are 5.32 and 2.97 eV, respectively. It suggests that the replacement of phenylene ring in **PPI** by thiophene leads to the destabilization of the HOMO level and the stabilization of the LUMO level. This is in agreement with finding in the cases of **PPV** and poly(thiophene vinylene) (**PTV**),[22] in which the calculated (IP, EA) of **PPV** and **PTV** are (5.21, 3.00) eV and (4.95, 3.34) eV, respectively.

Influence of the Aromatic Ring in the Polymer Backbone. Parameters of the optimized geometries and electronic structures of **PHTFI**, **PHTCI**, and **PHTNI** are also listed in Table 1. The replacement of the phenylene ring in **PHTPI** by the fluorene, carbazole or naphthalene unit has no influence on the bond length alternation (δ_r) and dihedral angle (Φ_1). However, it leads to a larger dihedral angle Φ_2. The Φ_2 of **PHTFI** and **PHTCI** are 26.0 ± 2.2 and 26.2 ± 5.7°, respectively, which are slightly larger than that of **PHTPI** at 24.0 ± 1.5°. However, the Φ_2 of **PHTNI** is 30.6 ± 0.4° and is larger than that of **PHTPI** by 6.6°. This indicates that the naphthalene substitution significantly enhances the nonplanarity of the poly(azomethine) backbone.

The calculated electronic structure parameters (IP, EA, E_g) of **PHTFI**, **PHTCI**, and **PHTNI** are (5.16, 2.74,

Table 2. Solubility,[a] the Molecular Weights, and Molecular Weight Distribution of the Poly(azomethine)s

	$CHCl_3$	THF	DMF	DMSO	NMP	*m*-cresol	toluene	$\bar{M}_w$	$\bar{M}_n$	PDI
PHTPI	+	++	++	++	++	+	+−	167700	51100	3.28
PHTFI[b]	−	+−	+−	+−	+	+−	−			
PHTCI	+−	++	++	++	++	+	+−	9800	5700	1.72
PHTNI	+−	++	+−	+−	++	+−	+−	2730	1380	1.98
PHTMOBPI	++	++	+−	+−	++	+	−	26610	9900	2.69

[a] Key: ++, soluble at room temperature; +, soluble on heating; +−, partially soluble on heating; −, insoluble. [b] Not soluble in THF and cannot be measured by GPC.

2.42 eV), (5.05, 2.38, 2.67 eV), and (5.16, 2.66, 2.50 eV), respectively. They exhibit asymmetric destabilization of the HOMO and LUMO levels in comparison with those of **PHTPI** (5.32, 2.97, 2.35 eV) due to the electron-donating substitution. However, **PHTFI**, **PHTCI**, and **PHTNI** have a larger E_g than **PHTPI**, which is due to the larger dihedral angle Φ_2, as described previously. The band gap of **PHTCI** is much larger than that of **PHTFI**, although they have a similar dihedral angle Φ_2. This may be attributed to the interruption of π-electron conjugation resulted from the introduction of the kink disorder of the 3,6-carbazole group in **PHTCI**.[32]

Influence of Electron Donor/Acceptor Substituents. The optimized geometries and electronic structures of **PHTMOBPI**, **PHTMOPI**, and **PHTNOPI** are also shown in Table 1. The presence of the side chain substituents is found to increase the lengths of the adjacent two C−C bonds (R_S in Table 1) within the phenylene rings to which they are connected, as compared with that of **PHTPI**. This is in agreement with the literature results on the cyano- or methoxy-substituted phenylenevinylene oligomers.[19f] As shown in Table 1, there is no significant influence on the bond length alternation (δ_r) when different electron-donating or electron-withdrawing side group is introduced to the parent material **PHTPI**. The dihedral angle Φ_1 of **PHTMOBPI**, **PHTMOPI**, and **PHTNOPI** are close to zero but Φ_2 shows a significant variation, which are 15.4 ± 4.1, 27.3 ± 1.6, and 38.6 ± 7.5°, respectively. The variation of the dihedral angle Φ_2 by the donor or acceptor substitution might be attributed to the interaction between the lone-pair electrons on the C=N nitrogen and the side-group substiuents.

The calculated electronic structures (IP, EA, E_g) of **PHTMOBPI**, **PHTMOPI**, and **PHTNOPI** are (5.25, 2.83, 2.42 eV), (5.29, 2.96, 2.33 eV), and (6.02, 3.36, 2.66 eV), respectively. As compared with **PHTPI** (5.32, 2.97, 2.35 eV), the substitution of electron-donating methoxy side group shows asymmetric destabilization of the HOMO and LUMO levels while the electron-withdrawing nitro side group shows asymmetric stabilization. The IP of both **PHTMOBPI** and **PHTMOPI** is smaller than that of **PHTPI** due to the methoxy electron-donating substitution. However, the band gap of **PHTMOBPI** is larger than that of **PHTMOPI** even though the latter has a larger dihedral angle Φ_2. This is probably accounted for by the twisting 36° angle between the two phenylene rings, which results from the steric hindrance by the ortho hydrogen atoms of *p*-biphenylene in **PHTMOBPI**. Besides, **PHTNOPI** has a larger band gap than **PHTPI**, which is due to the larger dihedral angle Φ_2.

In the case of **PHTNOPI**, which has a much larger dihedral angle Φ_2 than **PHTPI**, the extent of the stabilization of the LUMO level is smaller than that of the HOMO level, upon the substitution with a nitro group. This result is opposite to the literature results for **PPV** derivatives,[19c,19d] where the LUMO level was found to be more affected than the HOMO level upon the electron-accepting group substitution. The difference can be explained by the nonplanar conformation of the poly(azomethine)s, whereas **PPV** derivatives in the literature are considered to have a planar structure.

It is known that the decrease of planarity lowers the HOMO level but raises the LUMO level and thus leads to a larger band gap.[19a] Moreover, the degree of the mixing of the nitrogen lone-pair orbitals with both frontier orbitals increases with the dihedral angle Φ_2.[5d] Since the nitrogen lone-pair orbital is energetically more stable than the π-orbital, the extent of the stabilization of the HOMO and LUMO orbitals also increases with the dihedral angle Φ_2. Such characteristic makes the HOMO level more affected than the LUMO level upon the electron-accepting substitution in the poly(azomethine)s with nonplanar conformation.

Synthesis and Characterization. To verify the theoretical calculations on the seven poly(azomethine)s we tried to prepare and experimentally investigate them. The syntheses of **PHTPI**, **PHTFI**, **PHTCI**, **PHTNI**, and **PHTMOBPI** were successful, but that of **PHTNOPI** failed. The failure of the synthesis of **PHTNOPI** may be due to the poor reactivity of the thiophenic aldehyde toward nucleophilic attack than that of the aromatic aldehyde.[8f] In the case of **PHTMOPI**, the commercial diamine was not available and thus was not prepared.

Information about the solubility of the new poly(azomethine)s is given in Table 2. The polymers are partially or fully soluble in organic solvents, such as $CHCl_3$, THF, DMF, DMSO, NMP, toluene, or *m*-cresol at room temperature or on heating. The weight-average molecular weight ($\bar{M}_w$), number-average molecular weight ($\bar{M}_n$), and molecular weight distribution or polydispersity index ($\bar{M}_w/\bar{M}_n$,PDI) of the poly(azomethine)s are listed in Table 2. The moderate molecular weight may be attributed to the inferior reactivity of **DFHT** toward nucleophilic attack compared to the aromatic aldehyde,[8f] as described above. The molecular weight of **PHTFI** was not measured because of its poor solubility in THF.

Figure 2 shows the ^1H NMR spectrum of the monomer **DFHT** in $CDCl_3$, and the numbers of protons are in good agreement with the proposed structure. Signals in the ranges 0.89−3.02 and 9.98−10.15 ppm are assigned to the hexyl group and the two aldehyde protons, respectively. The peak at 7.66 ppm is assigned to the proton on the thiophene. The ^{13}C NMR spectrum of **DFHT** shows six resonance lines in the aliphatic region at 13.97, 22.45, 28.46, 28.83, 31.13, and 31.44 ppm assigned to the six different carbons of the hexyl group. The peaks at 137.14, 143.25, 147.83, and 151.98 ppm are due to the four carbons on the thiophene ring whereas the resonances at 182.96 and 183.35 ppm are assigned to the two carbons on the aldehyde group. The NMR results support the chemical structure of **DFHT** as proposed.

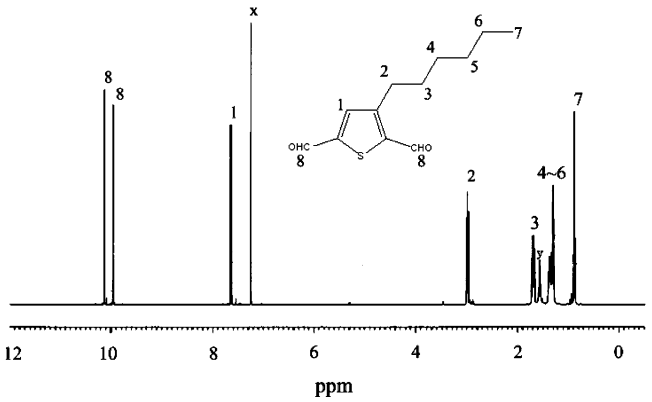

Figure 2. ^{1}H NMR spectrum of monomer **DFHT** (in $CDCl_3$): (x) $CHCl_3$; (y) H_2O.

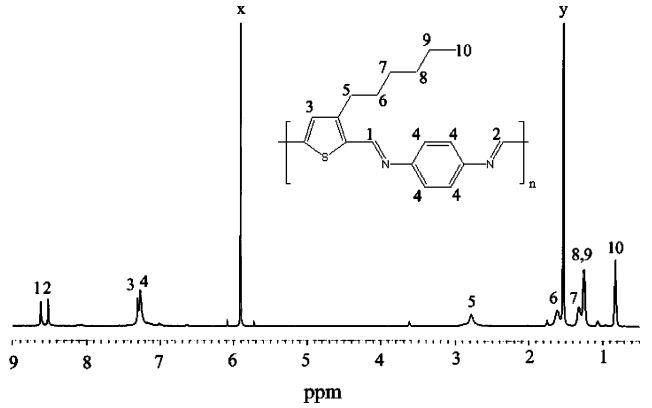

Figure 3. ^{1}H NMR spectrum of **PHTPI** (in 1,1,2,2-tetrachloroethane-d_2): (x) $C_2H_2Cl_4$; (y) H_2O.

Figure 3 shows the ^{1}H NMR spectrum of **PHTPI** in 1,1,2,2-tetrachloroethane-d_2. The chemical shifts of the imine proton resonances are observed at 8.52 and 8.62 ppm, which confirm the presence of the azomethine linkage. The protons on the phenylene and thiophene rings are around 7.27 and 7.31 ppm, respectively. The peaks located at 0.83, 1.25−1.60, and 2.78 ppm are attributed to alkyl side chain protons (methyl, methylenes, and α-CH_2, respectively). The FTIR spectra of the monomer **DFHT** and the poly(azomethine)s are shown in Figure 4. The most intense absorption band at 1591−1626 cm^{-1} in the polymers corresponds to the C=N stretching vibration of the imine moiety. The peaks attributed to the aliphatic C−H stretching vibration of the polymers are observed at 2855−2956 cm^{-1}. The absorption band at 1678 cm^{-1} corresponding to the aldehyde C=O stretching vibration in **DFHT** disappears in the spectra of **PHTPI**, **PHTFI**, **PHTCI**, and **PHTMOBPI**. However, the spectra of **PHTNI** and **PHTMOBPI** show residual aldehyde end groups due to their low molecular weights. Nevertheless, the NMR and FTIR results support the successful preparation of the poly(azomethine)s.

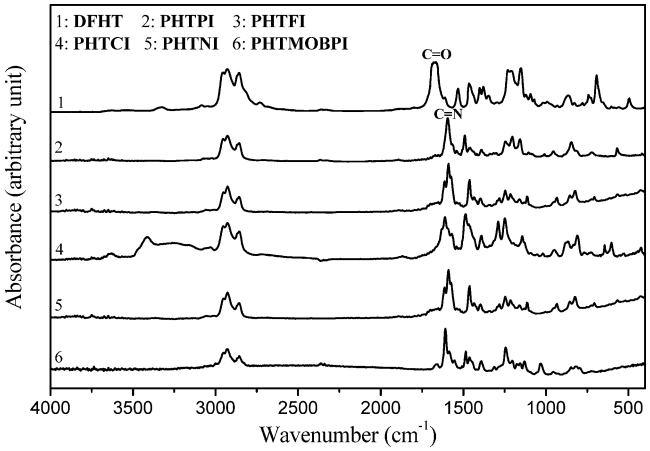

Figure 4. FTIR spectra of monomer **DFHT** and poly(azomethine)s.

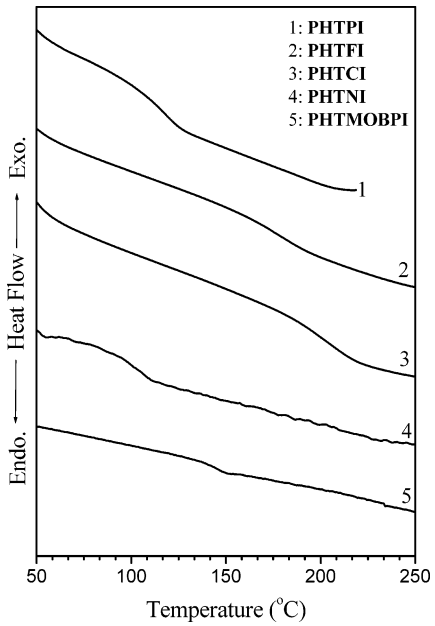

Figure 5. DSC curves of the synthesized poly(azomethine)s.

Properties of Poly(azomethine)s. From the TGA curves (not shown) of the poly(azomethine)s we determined the thermal decomposition temperatures (T_d) that are listed in Table 3. The polymers show fairly good thermal stability with T_d of 329−368 °C. Figure 5 shows the DSC curves of the five poly(azomethine)s. The glass transition temperatures (T_g) are listed in Table 3. No crystalline melting peak was seen in these polymers prior to decomposition. The polymers show a glass transition temperature in the range of 107−206 °C. The higher T_g of **PHTFI**, **PHTCI**, and **PHTNI** than that of **PHTPI** are due to the more rigid fluorene, carbazole, and naphthalene backbones, respectively.

Figure 6 shows the solution and thin film optical absorption spectra of the poly(azomethine)s in the

Table 3. Thermal, Absorption, and Emission Properties of the Poly(azomethine)s

	T_d (°C)	T_g (°C)	λ_{max}(solution) (nm)	λ_{max}(film) (nm)	λ_{max}^{PL}(solution) (nm)
PHTPI[a]	329	118	471	468	536
PHTFI[b]	336	174	474	483	573
PHTCI[a]	358	206	452	432	537
PHTNI[a]	368	145	439	463	542
PHTMOBPI[a]	359	107	453	464	533

[a] In THF. [b] In NMP.

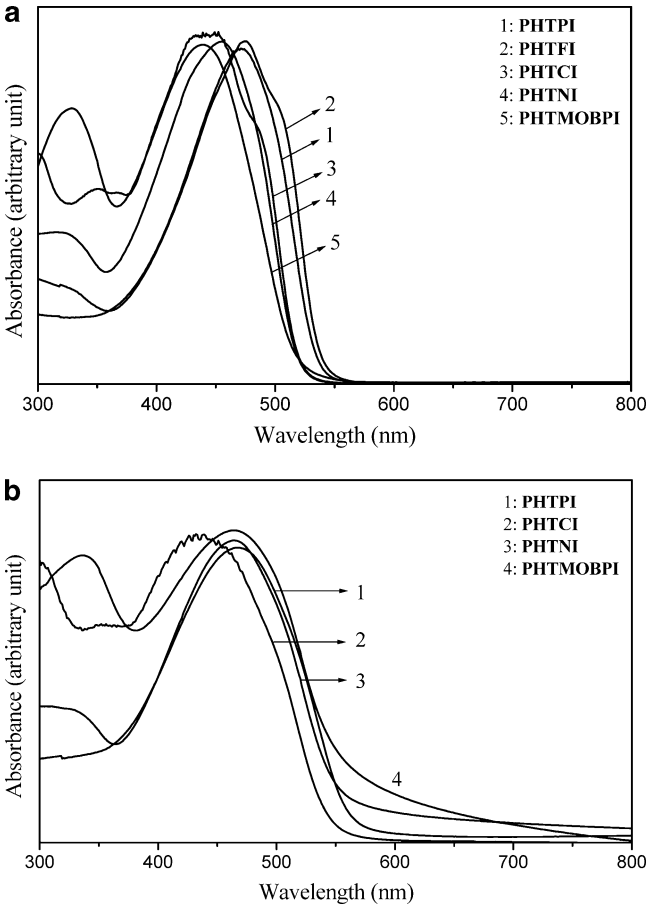

Figure 6. (a) Solution optical absorption spectra of poly(azomethine)s. (b) Thin film optical absorption spectra of poly(azomethine)s.

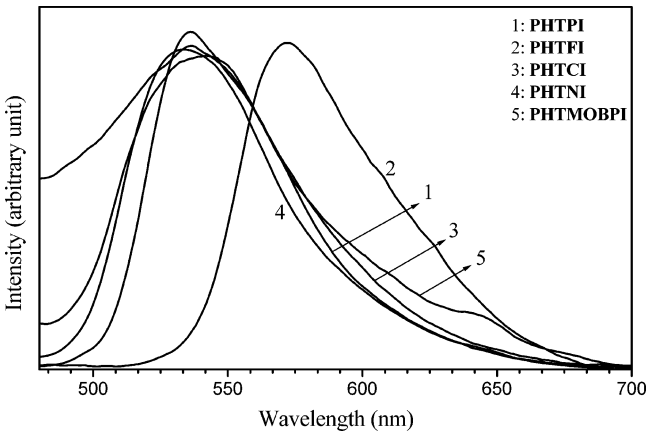

Figure 7. Solution photoluminescence emission spectra of poly(azomethine)s (excited at 430 nm).

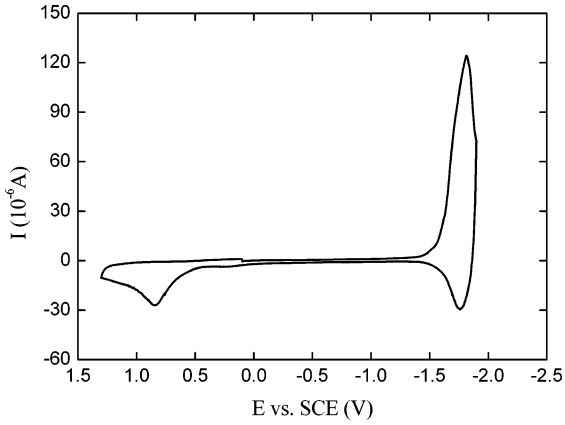

Figure 8. Cyclic voltammogram of **PHTMOBPI** thin film.

wavelength range of 300−800 nm. All the polymers strongly absorb visible light. The absorption maxima (λ_{max}) of the polymers in solution and as thin films are 439−474 and 432−483 nm, respectively, as shown in Table 3. The solution and thin film absorption maxima of PHTPI are the same, indicating that the conformations in solution and the solid state are identical. Small increases in the absorption maxima are observed in going from solution to thin films for all the other poly(azomethine)s except **PHTCI**. The increase in absorption maximum is consistent with increased planarity of the chain in the solid state. The band gaps of the polymer films obtained from the optical absorption edge are in the range of 2.21−2.28 eV, which are in good agreement with the theoretical results. The poly(azomethine)s exhibit smaller band gaps than the parent **PPI** with E_g of 2.50 eV.[5a] The optical band gaps of **PHTCI**, **PHTNI**, and **PHTMOBPI** are larger than that of **PHTPI** due to the larger dihedral angle of the polymer backbone as described previously. The photoluminescence (PL) emission spectra (excited at 430 nm) of the polymers in solution are shown in Figure 8, and the corresponding emission maxima (λ_{max}^{PL}) are listed in Table 3. The emission maxima are in the range 533−573 nm, which are strongly red-shifted from their optical absorption maximum. However, the measured PL quantum efficiency of the present conjugated poly(azomethine)s was less than 0.03%. The poor emission efficiency of the conjugated poly(azomethine)s is similar to those of oligothienylene based poly(azomethine)s[8e] and **MEH−PPI**.[11] The PL emission properties of the poly(azomethine)s are thus inferior compared to poly(arylenevinylene)s[1,33] or polyfluorenes.[34]

The reduction and oxidation potentials of the poly(azomethine)s were investigated by cyclic voltammetry. Figure 8 shows the cyclic voltammogram of **PHTMOBPI**. It shows that **PHTMOBPI** exhibits a quasi reversible reduction. A similar electrochemical reduction was also found in **PHTPI** but the others do not show reversible reduction. The electrochemical

Table 4. Electrochemical Properties of Poly(azomethine)s

	oxidation (vs SCE)				reduction (vs SCE)					
	E_{pc}[a] (V)	E_{pa} (V)	E_{onset} (V)	IP (eV)	E_{pc} (V)	E_{pa}[a] (V)	E_{onset} (V)	EA (eV)	E_g^{ec}[b] (eV)	E_g^{opt}[c] (eV)
PHTPI		1.03	0.86	5.26	−1.84	−1.54	−1.27	3.13	2.13	2.21
PHTFI		1.08	0.77	5.23	−1.53		−1.32	3.08	2.15	*d*
PHTCI		1.12	0.73	5.17	−1.75		−1.37	3.03	2.19	2.28
PHTNI		1.25	0.97	5.37	−1.54		−1.26	3.14	2.23	2.26
PHTMOBPI		0.84	0.64	5.04	−1.82	−1.76	−1.60	2.80	2.24	2.25

[a] The E_{pc} of oxidation of all polymers and that of reduction of **PHTFI**, **PHTCI**, and **PHTNI** are not reversible. [b] The elecrochemical band gap, E_g^{ec} = IP − EA. [c] The optical band gap is from the absorption edge of the thin film, E_g^{opt} (eV) = 1240/λ_{edge} (nm). [d] Not available due to solubility.

oxidation of all the polymers was not reversible under the conditions of our experiments. The electrochemical reduction and oxidation potentials and the electronic structure parameters of all the polymers are given in Table 4. The onset potentials (E_{onset}) of oxidation and reduction for **PHTPI** are observed at +0.86 and −1.27 eV, respectively, which correspond to an IP value of 5.26 eV and an EA value of 3.13 eV. When the phenylene ring (**PHTPI**) in the main chain was replaced by the fluorene (**PHTFI**) or carbazole (**PHTCI**) unit, the IP decreased only slightly. The electrochemical band gap of **PHTCI** was larger than those of **PHTPI** and **PHTFI**, which is attributed to the interruption of the linearity of the conjugated backbone. It is consistent with the theoretical calculation as discussed previously. A similar trend is shown in Table 4 on the effect of backbone planarity on the electronic properties by comparing **PHTNI** with **PHTPI**. Moreover, side-group substitution such as electron-donating group (e.g., **PHTMOBPI**) also causes a difference in electrochemical behavior. These trends on the effects of substitution of backbone ring or side chain on the electronic properties as determined by electrochemical characterization are in good agreement with the theoretical calculations and optical absorption results.

Conclusions

We presented a joint theoretical and experimental investigation of new thiophene-based conjugated poly(azomethine)s. The theoretical analysis showed that the thiophene-based poly(azomethine)s have smaller band gaps in comparison with the parent **PPI**. The theoretical calculations showed that substitution of backbone ring with electron-donating or withdrawing side group significantly affects the backbone planarity and thus results in the variation of the electronic properties, including ionization potential, electronic affinity and band gap. For comparison with the theoretical electronic properties we synthesized and investigated five new soluble conjugated poly(azomethine)s. The experimentally observed effects of the backbone ring or side chain on the electronic properties were in a good agreement with the theoretical results. The results of this study demonstrate that the electronic properties of conjugated poly(azomethine)s are tunable through the backbone ring or side chain, which could be important for electronic or optoelectronic applications.

Acknowledgment. The work at National Taiwan University was supported by the National Science Council, the Ministry of Education, and the Ministry of Economic Affairs of Taiwan, R.O.C. That at the University of Washington was supported by the Air Force Office of Scientific Research (Grant F49620-03-1-0162).

Supporting Information Available: Tables of optimum geometry data for **PPI**, **PHTPI**, **PHTFI**, **PHTCI**, **PHTNI**, **PHTMOBPI**, **PHTMOPI**, and **PHTNOPI** and figures showing the ^{13}C NMR spectrum of **DFHT** and cyclic voltammograms of **PHTPI**, **PHTFI**, **PHTCI**, and **PHTNI**. This material is available free of charge via the Internet at http://pubs.acs.org.

References and Notes

(1) (a) Kraft, A.; Grimsdale, A. C.; Holmes, A. B. *Angew. Chem., Int. Ed. Engl.* **1998**, *37*, 402. (b) Gross, M.; Müller, D. C.; Nothofer, H. G.; Scherf, U.; Neher, D.; Bräuchle, C.; Meerholz, K. *Nature* **2000**, *405*, 661. (c) Zhang, X.; Shetty, A. S.; Jenekhe, S. A. *Macromolecules* **1999**, *32*, 7422. (d) Zhang, X.; Jenekhe, S. A. *Macromolecules* **2000**, *33*, 2069.

(2) (a) Bao, Z.; Dodabalapur, A.; Lovinger, A. J. *Appl. Phys. Lett.* **1996**, *69*, 4108. (b) Sirringhaus, H.; Tessler, N.; Friend, R. H. *Science* **1998**, *280*, 1741. (c) Babel, A.; Jenekhe, S. A. *J. Am. Chem. Soc.* **2003**, *125*, 13656. (d) Babel, A.; Jenekhe, S. A. *Adv. Mater.* **2002**, *14*, 371. (e) Babel, A.; Jenekhe, S. A. *J. Phys. Chem. B* **2003**, *107*, 1749.

(3) (a) Halls, J. J. M.; Walsh, C. A.; Greenham, N. C.; Marseglia, E. A.; Friend, R. H.; Moratti, S. C.; Holmes, A. B. *Nature* **1995**, *376*, 498. (b) Yu, G.; Gao, J.; Hummelen, J. C.; Wudl., F.; Heeger, A. J. *Science* **1995**, *270*, 1789. (c) Antoniadis, H.; Hsieh, B. R.; Abkowitz, M. A.; Jenekhe, S. A.; Stolka, M. *Synth. Met.* **1994**, *62*, 265. (d) Jenekhe, S. A.; Yi, S. *Appl. Phys. Lett.* **2000**, *77*, 2635. (e) Alam, M. M.; Jenekhe, S. A. *Chem. Mater.* **2004**, *16*, 4647.

(4) Morgan, P. W.; Kwolek, S. L.; Pletcher, T. C. *Macromolecules* **1987**, *20*, 729.

(5) (a) Yang, C. J.; Jenekhe, S. A. *Chem. Mater.* **1991**, *3*, 878. (b) Yang, C. J.; Jenekhe, S. A. *Chem. Mater.* **1994**, *6*, 196. (c) Yang, C. J.; Jenekhe, S. A. *Chem. Mater.* **1995**, *7*, 1276. (d) Yang, C. J.; Jenekhe, S. A. *Macromolecules* **1995**, *28*, 1180. (e) Yang, C. J.; Jenekhe, S. A.; Meth, J. S.; Vanherzeele, H. *Ind. Eng. Chem. Res.* **1999**, *38*, 1759.

(6) Tatsuura, S.; Sotoyama, W.; Motoyoshi, K.; Matsuura, A.; Hayano, T.; Yoshimura, T. *Appl. Phys. Lett.* **1993**, *62*, 2182.

(7) Park, S. B.; Kim, H.; Zin, W. C.; Jung, J. C. *Macromolecules* **1993**, *26*, 1627.

(8) (a) Destri, S.; Porzio, W.; Dubitsky, Y. *Synth. Met.* **1995**, *75*, 25. (b) Destri, S.; Porzio, W.; Dubitsky, Y. *Synth. Met.* **1995**, *69*, 287. (c) Olinga, T. E.; Destri, S.; Botta, C.; Porzio, W.; Consonni, R. *Macromolecules* **1998**, *31*, 1070. (d) Destri, S.; Khotina, I. A.; Porzio, W. *Macromolecules* **1998**, *31*, 1079. (e) Destri, S.; Khotina, I. A.; Porzio, W.; Botta, C. *Opt. Mater.* **1998**, *9*, 411. (f) Pasini, M.; Pelizzi, C.; Porzio, W.; Predieri, G.; Vignali, C. *Macromolecules* **1999**, *32*, 353.

(9) (a) Wang, C.; Xie, X.; LeGoff, E.; Albritton-Thomas, J.; Kannewurf, C. R.; Kanatzidis, M. G. *Synth. Met.* **1995**, *71*, 74. (b) Wang, C.; Shieh, S.; LeGoff, E.; Kanatzidis, M. G. *Macromolecules* **1996**, *29*, 3147.

(10) Matsumoto, T.; Yamada, F.; Kurosaki, T. *Macromolecues* **1997**, *30*, 3547.

(11) Thomas, O.; Inganäs, O.; Anderson, M. R. *Macromolecules* **1998**, *31*, 2676.

(12) Miyaji, T.; Azuma, C.; Asaoka, E.; Nakamura, S. *J. Polym. Sci., Polym. Chem.* **2000**, *38*, 1064.

(13) Grigoras, M.; Catanescu, C. O.; Colotin, G. *Macromol. Chem. Phys.* **2001**, *202*, 2262.

(14) (a) Kim, J. J.; Kim, K. S.; Baek, S.; Kim, H. C.; Ree, M. *J. Polym. Sci., Polym. Chem.* **2002**, *40*, 1173. (b) Kim, H. C.; Kim, J. S.; Kim, K. S.; Park, H. K.; Baek, S.; Ree, M. *J. Polym. Sci., Polym. Chem.* **2004**, *42*, 825.

(15) Krebs, F. C.; Jorgensen, M. *Synth. Met.* **2004**, *142*, 181.

(16) (a) Kimoto, A.; Cho, J.; Higuchi, M.; Yamamoto, K. *Macromolecules* **2004**, *37*, 5531. (b) Skene, W. G. *Polym. Prepr.*. **2004**, *45*, 254.

(17) (a) Roncali, J. *Chem. Rev.* **1997**, *97*, 173. (b) van Mullekom, H. A. M.; Vekemans, J. A. J. M.; Havinga, E. E.; Meijer, E. W. *Mater. Sci. Eng.* **2001**, *32*, 1.

(18) (a) Springborg, M.; Schmidt, K.; Meifer, H.; de Maria, L. In *Organic Electronic Materials: Conjugated Polymers and Low Molecular Weight Organic Solids*; Farchioni, R., Grosso, G., Eds.; Springer: New York, 2001; pp 39−87. (b) Hutchison, G. R.; Zhao, Y. J.; Delley, B.; Freeman, A. J.; Ratner, M. A.; Marks, T. J. *Phys. Rev. B* **2003**, *68*, 035204. (c) Yang, S.; Olishevski, P.; Kertesz, M. *Synth. Met.* **2004**, *141*, 171.

(19) (a) Brédas, J. L.; Street, G. B.; Thémans, B.; André, J. M. *J. Chem. Phys.* **1985**, *83*, 1323. (b) Toussaint, J. M.; Bredas, J. L. *Macromolecules* **1993**, *26*, 5240. (c) Brédas, J. L.; Heeger, A. J. *Chem. Phys. Lett.* **1994**, *217*, 507. (d) Cornil, J.; dos Santos, D. A.; Beljonne, D.; Brédas, J. L. *J. Phys. Chem.* **1995**, *99*, 5604. (e) Zojer, E.; Pogantsch, A.; Hennebicq, E.; Beljonne, D.; Bredas, J. L.; de Freitas, P. S.; Scherf, U.; List, E. J. W. *J. Phys. Chem.* **2002**, *117*, 6794. (f) Cornil, J.; Gueli, I.; Dkhissi, A.; Sancho-Garcia, J. C.; Hennebicq, E.; Calbert, J. P.; Lemaur, V.; Beijonne, D.; Brédas, J. L. *J. Chem. Phys.* **2003**, *118*, 6615.

(20) (a) Kertesz, M.; Lee, Y. S. *J. Phys. Chem.* **1987**, *91*, 2690. (b) Lee, Y. S.; Kertesz, M. *J. Chem. Phys.* **1988**, *88*, 2609. (c) Hong, S. Y.; Kertesz, M.; Lee, Y. S.; Kim, O. K. *Chem. Mater.* **1992**, *4*, 378. (d) Hong, S. Y.; Kertesz, M.; Lee, Y. S.; Kim, O. K. *Macromolecules* **1992**, *25*, 5424. (e) Choi, C. H.; Kertesz, M. *J. Chem. Phys.* **1997**, *107*, 6712.

(21) Chen, W. C.; Liu, C. L.; Yen, C. T.; Tsai, F. C.; Tonzola, C. J.; Olson, N.; Jenekhe, S. A. *Macromolecules* **2004**, *37*, 5959.
(22) Eckhardt, H.; Shacklette, L. W.; Jen, K. Y.; Elsenbaumer, R. L. *J. Chem. Phys.* **1989**, *91*, 1303.
(23) (a) Salzner, U.; Pickup, P. G.; Poirier, R. A.; Lagowski, L. B. *J. Phys. Chem. A* **1998**, *102*, 2572. (b) Salzner, U.; Lagowski, L. B.; Pickup, P. G.; Poirier, R. A. *Synth. Met.* **1998**, *96*, 177.
(24) (a) Kwon, O.; McKee, M. L. *J. Phys. Chem. A* **2000**, *104*, 7106. (b) Kwon, O.; McKee, M. L. *J. Phys. Chem. B* **2000**, *104*, 1686.
(25) Tachibana, M.; Tanaka, S.; Yamashita, Y.; Yoshizawa, K. *J. Phys. Chem. B* **2002**, *106*, 3549.
(26) Hutchison, G. R.; Ratner, M. A.; Marks, T. J. *J. Phys. Chem. A* **2002**, *106*, 10596.
(27) Brière, J. F.; Côté, M. *J. Phys. Chem. B* **2004**, *108*, 3123.
(28) Frisch, M. J.; Trucks, G. W.; Schlegel, H. B.; Scuseria, G. E.; Robb, M. A.; Cheeseman, J. R.; Montgomery, J. A., Jr.; Vreven, T.; Kudin, K. N.; Burant, J. C.; Millam, J. M.; Iyengar, S. S.; Tomasi, J.; Barone, V.; Mennucci, B.; Cossi, M.; Scalmani, G.; Rega, N.; Peterssonp, G. A.; Nakatsuji, H.; Hada, M.; Ehara, M.; Toyota, K.; Fukuda, R.; Hasegawa, J.; Ishida, M.; Nakajima, T.; Honda, Y.; Kitao, O.; Nakai, H.; Klene, M.; Li, X.; Knox, J. E.; Hratchian, H. P.; Cross, J. B.; Adamo, C.; Jaramillo, J.; Gomperts, R.; Stratmann, R. E.; Yazyev, O.; Austin, A. J.; Cammi, R.; Pomelli, C.; Ochterski, J. W.; Ayala, P. Y.; Morokuma, K.; Voth, G. A.; Salvador, P.; Dannenberg, J. J.; Zakrzewski, V. G.; Dapprich, S.; Daniels, A. D.; Strain, M. C.; Farkas, O.; Malick, D. K.; Rabuck, A. D.; Raghavachari, K.; Foresman, J. B.; Ortiz, J. V.; Cui, Q.; Baboul, A. G.; Clifford, S.; Cioslowski, J.; Stefanov, B. B.; Liu, G.; Liashenko, A.; Piskorz, P.; Komaromi, I.; Martin, R. L.; Fox, D. J.; Keith, T.; Al-Laham, M. A.; Peng, C. Y.; Nanayakkara, A.; Challacombe, M.; Gill, P. M. W.; Johnson, B.; Chen, W.; Wong, M. W.; Gonzalez, C.; Pople, J. A. Gaussian Inc.: Pittsburgh, PA, 2003.
(29) Mitsumori, T.; Inoue, K.; Koga, N.; Iwamura, H. *J. Am. Chem. Soc.* **1995**, *117*, 2467.
(30) Eaton, D. F. *Pure Appl. Chem.* **1988**, *60*, 1107.
(31) (a) Agrawal, A. K.; Jenekhe, S. A. *Chem. Mater.* **1996**, *8*, *579*. (b) Kulkarni, A. P.; Tonzola, C. J.; Babel, A.; Jenekhe, S. A. *Chem. Mater.* **2004**, *16*, 4556.
(32) Xia, C. J.; Advincula, R. C. *Macromolecules* **2001**, *34*, 5854.
(33) Alam, M. M.; Jenekhe, S. A. *Chem. Mater.* **2002**, *14*, 4775.
(34) (a) Teetsov, J.; Fox, M. A. *J. Mater. Chem.* **1999**, *9*, 2117. (b) Kulkarni, A. P.; Kong, X.; Jenekhe, S. A. *J. Phys. Chem. B* **2004**, *108*, 8689. (c) Lin, W. J.; Chen, W. C.; Wu, W. C.; Niu, Y-H.; Jen, A. K. Y. *Macromolecules* **2004**, *37*, 2335.

MA048112O